Mon. Not. R. Astron. Soc. **000**, 1–11 (2011) Printed 20 February 2012 (MN LATEX style file v2.2)

High frequencies in the δ Scuti star KIC 4840675

L. A. Balona[1], M. Breger[2], G. Catanzaro[3], M. S. Cunha[4], A. Grigahcène[4], G. Handler[5], Z. Kołaczkowski[6], D. W. Kurtz[7], S. Murphy[7], E. Niemczura[6], M. Paparo[9], B. Smalley[8], R. Szabo[9], K. Uytterhoeven[10]

[1]*South African Astronomical Observatory, P.O. Box 9, Observatory 7935, Cape Town, South Africa*
[2]*Department of Astronomy, University of Texas, Austin, TX 78712, USA*
[3]*INAF - Osservatorio Astrofisico di Catania, Via S. Sofia 78, I95123, Catania, Italy*
[4]*Centro de Astrofísica and Faculdade de Ciências, Universidade do Porto, Rua das Estrelas, 4150-762 Porto, Portugal*
[5]*Nicolaus Copernicus Astronomical Center, Bartycka 18, 00-716 Warsaw, Poland*
[6]*Astronomical Institute, Wrocław University, Kopernika 11, 51-622 Wrocław, Poland*
[7]*Jeremiah Horrocks Institute, University of Central Lancashire, Preston PR1 2HE, UK*
[8]*Astrophysics Group, Keele University, Staffordshire, ST5 5BG UK*
[9]*Konkoly Observatory MTA CSFK, H-1121, Konkoly-Thege u. 15-17, Budapest, Hungary*
[10]*Instituto de Astrofsica de Canarias, 38200 La Laguna, Tenerife, Spain*

ABSTRACT
We show that the star KIC 4840675 observed by *Kepler* is a triple system with a rapidly-rotating A-type star and two solar-type fainter companions. The A-type star is a δ Scuti variable with a dominant mode and many other modes of lower amplitude, including several low-frequency variations. The low-frequency variation with highest amplitude can be interpreted as rotational modulation with the light curve changing with time. However, the most interesting aspect of this star is a triplet of independent modes in the range 118–129 d^{-1} (1.4–1.5 mHz), which is far outside the range of typical δ Scuti frequencies. We discuss the possibility that these modes could be solar-like oscillations, oscillations of the roAp type or due to an unseen pulsating compact companion.

Key words: asteroseismology – pulsation – stars: binaries: spectroscopic – stars: individual: KIC 4840675 – stars: oscillations – stars: variables: δ Scuti

1 INTRODUCTION

The δ Scuti variables are dwarfs or giants with spectral types between A2 and F5 and frequencies in the range 5–50 d^{-1}. Most of the pulsational driving in these stars is by the κ mechanism operating in the He II partial ionization zone. In the cooler δ Sct stars, much of the driving is due to the convective blocking mechanism (Guzik et al. 2000), which is also the principal source of driving for the γ Dor stars. The excited modes are radial or nonradial p modes or mixed modes of the p and g type. There is no known example of a star with frequencies typical of δ Sct stars and also with the high frequencies associated with roAp stars. Most δ Scuti stars do not pulsate at frequencies higher than about 50 d^{-1} (Balona & Dziembowski 2011).

The Ap stars are slowly rotating, chemically peculiar A–F type stars with non-uniform distributions of chemical elements, both laterally across the surface and vertically in the atmosphere. The chemical peculiarity is thought to be due to diffusion of elements in a strong magnetic field (Michaud 1970). The axis of the magnetic field in these stars is tilted with respect to the axis of rotation. A small number of the cooler Ap stars have been found to pulsate with periods of 3–24 minutes (frequencies of 60–500 d^{-1} or 0.7–5.5 mHz). These are the roAp stars (Kurtz 1982). The mechanism that drives the pulsations is not known, but could be the κ mechanism operating in the H ionization zone in regions of the star where convection has been suppressed (Balmforth et al. 2001). It is thought that diffusion in the strong magnetic field of an Ap star will deplete He from the driving zone which therefore tends to suppress the δ Sct pulsations. Energy losses from magneto-acoustic coupling also tends to dampen these modes in Ap stars (Saio 2005). However, the Ap star HD 21190 (F2III SrEuSi) does pulsate with a frequency of 6.68 d^{-1}, but other frequencies are probably present (Koen et al. 2001). The star is the most evolved Ap star known which may be a clue to why it pulsates.

Space missions, such as *MOST, CoRoT* and *Kepler*, have been extremely successful in extending our understanding of stellar pulsations. KIC 4840675 (2MASS J19325792+3958452; RA = 19:32:58, Dec = +39:58:45) has

been observed by the *Kepler* satellite and listed as a δ Scuti variable by Uytterhoeven et al. (2011). There is no spectral type or spectroscopy of any kind available from the literature. From the *Kepler* Input Catalogue (KIC, Brown et al. (2011)), Kp = 9.67 mag, $T_{\rm eff}$ = 7100 K, $\log g$ = 3.55 and [Fe/H] = -0.2. Recently, Pinsonneault et al. (2011) have re-examined the KIC temperature scale and find that the KIC temperatures are too cool by about 100 K, but this result applies to stars with effective temperatures in the region 6000–7000 K. The KIC effective temperature for KIC 4840675 may also be somewhat too cool. We will show that the star has multiple components which in any case renders the photometric temperature rather ambiguous.

In addition to pulsations typical of δ Sct stars, the periodogram of this star shows a few low-amplitude peaks at around 120 $\rm d^{-1}$ (1300 μHz or a period of about 12 min). Such high frequencies are unknown in any other δ Sct star. In some δ Sct stars, harmonics of a dominant mode sometimes do have frequencies approaching this value, but these are not independent modes. The presence of such high frequencies in a δ Sct star calls to mind the possibility that it might be an Ap star and that the high frequencies are roAp pulsations. Alternatively, there is a possibility that the high frequencies could be solar-like oscillations excited by stochastic convective motions or perhaps arise in an unseen compact companion.

In this paper we show that KIC 4840675 is composed of at least three stars. The most luminous component is a rapidly-rotating A star which is the most probable source of the δ Sct pulsations. The other two stars appear to be similar to the Sun. We discuss the frequencies of the δ Sct component. The dominant low frequency may be the rotational frequency of the star. Finally, we attempt to locate the origin of the rapid light variation and the mechanism which drives these pulsations.

2 THE *KEPLER* PHOTOMETRY

The *Kepler* photometric observations mostly have exposures of about 30 min (long-cadence, LC), but some stars were observed in short-cadence (SC) mode in which the exposure time is about 1 min. Characteristics of SC data are described in Gilliland et al. (2010), while Jenkins et al. (2010) describe the characteristics of LC data. LC data are available for quarters 0–9, most of which are in the public domain except. Since the Nyquist frequency for LC data is only about 24 $\rm d^{-1}$, these data are of limited use for our purposes. KIC 4840675 was first observed in SC mode in the last part of quarter 3 and for the whole of quarter 9 (see Table 1 for a log of the observations).

The *Kepler* photometry is available as calibrated (but processed) and uncalibrated data. We used only the uncalibrated data. The SC light curve was examined and outliers removed. There are small magnitude jumps between different data sets which were adjusted by visual inspection. Part of the light curve (from Q3.3) is shown in Fig 1. Periodograms of the combined data are shown in Fig. 2. Note, in particular, the presence of three peaks in the region around 120 $\rm d^{-1}$. It is these high frequencies which have motivated this paper.

It is important to understand the source of these high

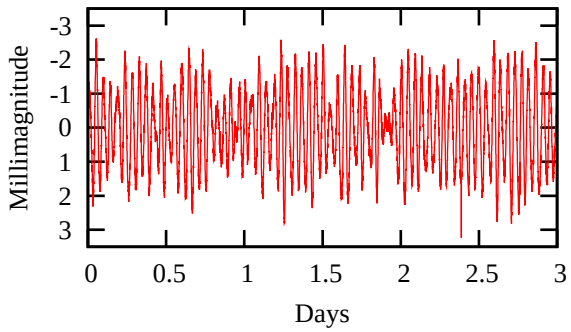

Figure 1. Part of the *Kepler* light curve of KIC 4840675.

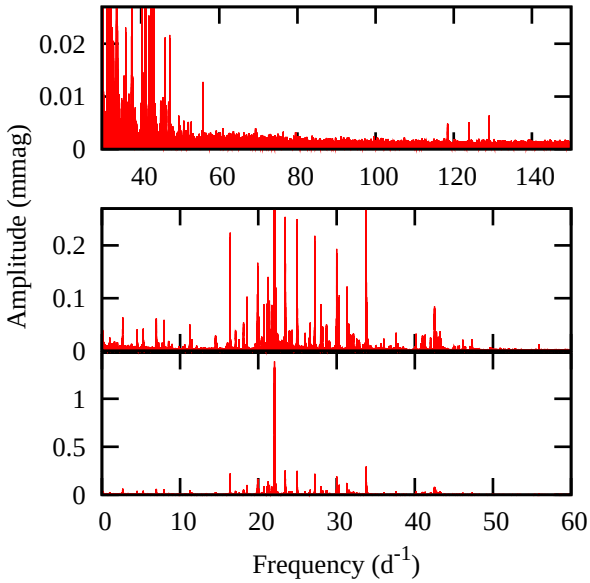

Figure 2. Periodograms of the combined data for KIC 4840675. The bottom panel shows the dominant frequency f_1 = 22.069 $\rm d^{-1}$. The middle panel shows the same part of the periodogram on an expanded scale. The top panel shows the outlying high-frequency triplet.

Table 1. Log of *Kepler* short-cadence observations for KIC 4840675. The *Kepler* quarter name, the start and ending truncated Julian day, the duration and the number of data points, N, are shown.

Quarter	Julian day	Days	N
Q3.3	55156.5 - 55182.5	26.0	38047
Q9.1	55641.5 - 55677.9	36.4	53320
Q9.2	55678.6 - 55707.1	28.5	41748
Q9.3	55707.8 - 55738.9	31.2	45609

frequencies as it may have its origins in a fainter star within the same aperture. For this purpose, we made a thorough check at the pixel level using the Q9.3 SC target pixel data. First, we checked the light curves of all available pixels within the downloaded region. None of the individual pixels show the high frequency triplet above the noise level. This is a strong indication that there is no close contaminator within the spatial resolution of *Kepler* that shows these high-frequency variations. In order to be detected when all the pixels are summed, any pixel would have to vary with large amplitude at these frequencies. There are two fainter stars within the downloaded region, but these are well separated from KIC 4840675. These stars also do not exhibit the frequencies in question.

Saturation will occur for such a bright target, but the total flux is preserved which allows for precise photometry. However, we noticed that the saturated pixels have a strange nonlinear variation. Instead of a constant saturated flux, saturation seems to occur at discrete flux levels. The jumps between these levels appear to be random. The mean flux in the optimal aperture is 1.88×10^6 e and the flux difference between the levels is about 50 e, so the relative variation is similar to the amplitudes of the three high frequencies. In addition, because the time interval varies between successive saturation level jumps, one needs to consider whether this frequency modulation may cause spurious side frequencies (Benkő et al. 2011). The irregular frequency modulation is hard to treat analytically, so we created an artificial data set containing only the flux jumps and averaged out the pulsation. We found no significant peaks in the relevant frequency region of the periodogram resulting from this simulation. It is not clear whether these jumps reflect a real charge distribution or a result of the readout process or other instrumental effect. Most probably this behavior averages out when the flux of all the pixels is summed, because the jumps do not occur at the same time in all pixels.

Another possibility which needs to be considered is that the high frequencies are of instrumental origin. This can be ruled out as none of these frequencies appear in the list of spurious frequencies in *Kepler* data by Baran (2012), nor do they appear in the periodograms of any of the over 2000 stars observed in SC mode and analysed by one of us (LAB). We conclude that the high frequencies are not an instrumental effect nor do they originate in any faint star within the aperture. They are almost certainly caused by a variation in one of the stars in the KIC 4840675 system.

3 SPECTROSCOPY

A single medium-resolution optical spectrum of KIC 4840675 was obtained using the cross-dispersed, Fibre-fed Échelle Spectrograph (FIES) attached to the Nordic Optical Telescope (NOT). The wavelength range is 3700–7300 Å, with a spectral resolution of 46 000 and a signal-to-noise ratio of about 100 at 5500 Å. The spectrum was reduced using `FIEStool` and consists of bias subtraction, scattered light correction, division by a normalized flat field and wavelength calibration. The continuum was normalized using `SPLAT`, the spectral analysis tool from the `Starlink` project (Draper et al. 2005).

It is clear from inspection of the spectrum that the lines

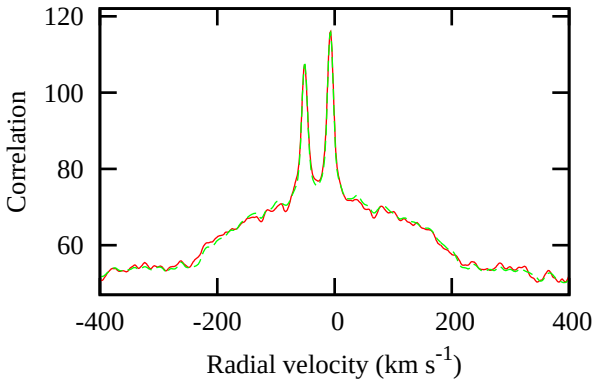

Figure 3. Cross-correlation between the observed spectrum and a synthetic template spectrum over the wavelength range 4950–5810 Å. The dashed curve is the cross-correlation with the best-fitting synthetic composite spectrum.

are broad, but there are many, weaker, sharp lines. Both the Mg b and Ca K lines are consistent with $\log g \approx 4.0 \pm 0.5$ dex. To analyze this spectrum, we generated synthetic spectra using the `spectrum` code (Gray 2010) and model atmospheres by Castelli et al. (1997). Cross-correlation of the observed spectrum with an unbroadened synthetic spectrum as template ($T_{\rm eff}$ = 7000 K, $\log g$ = 4.00 and solar metallicity) shows that there are at least three stars in the system (Fig. 3). There is one broad-lined component and two other stars with sharp lines. The cross-correlation enables us to obtain the radial velocity of each component in the system.

We need to determine the stellar parameters of all three stars given the spectrum and constraints imposed by the relative brightnesses. Our approach is to assume initial values and iterate until we converge to the best solution. We started by ignoring the two faint components B and C and assuming that the spectrum is due only to the bright A component. From the broad peak in the cross-correlation function, we estimated $v \sin i \approx 220\,{\rm km\,s^{-1}}$ for star A. This estimate was obtained after several trials in which the synthetic spectrum was broadened by different amounts. The above value is the best fit in matching the broad peak in the synthetic cross-correlation function with the broad peak in the observed cross-correlation function.

We created a grid of synthetic spectra with solar abundances, $v \sin i = 220\,{\rm km\,s^{-1}}$ and $6000 \leqslant T_{\rm eff} \leqslant 10000$ K in steps of 250 K and $2.5 \leqslant \log g \leqslant 5.0$ in steps of 0.5 dex. We fitted the Hα (6500–6620 Å) and Hβ (4800–4930 Å) line profiles to these models to estimate the effective temperature and surface gravity of the A component. The best match occurs for $T_{\rm eff} \approx 7250$ K and $\log g \approx 3.5$. Using the above parameters for star A and assumed values of $T_{\rm eff} = 6000$ K, $\log g = 4.5$ for components B and C, we generated synthetic combined spectra. For this purpose, we used the radial velocities derived from cross-correlation and initial guesses for the relative brightnesses and line broadenings. By comparing the cross-correlation function of the combined synthetic spectrum with the observed cross-correlation function (using the same template), we can adjust the relative brightnesses of the three components until we obtain a good match for the relative heights of the three peaks.

With improved relative brightnesses obtained in this

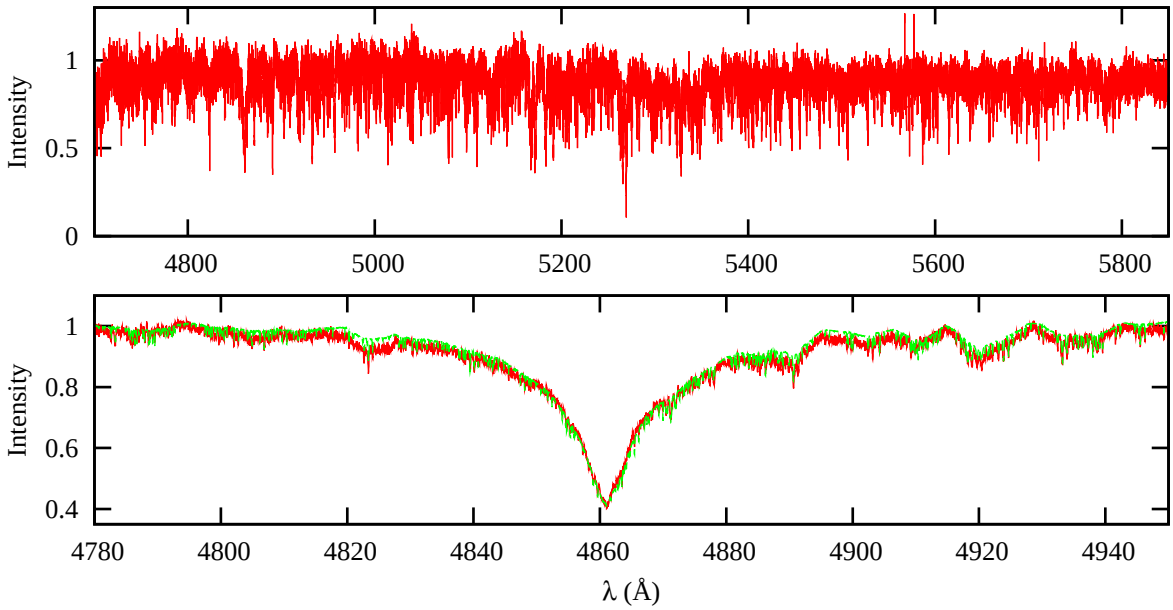

Figure 4. Bottom panel: the observed spectrum around Hβ (red) and the best fitting synthetic spectrum (green) with $T_{\rm eff} = 7400$ K, $\log g = 4.0$. Top panel: residual spectrum after subtracting this synthetic spectrum showing lines from the cooler, fainter, components.

way, we repeated the process of matching the Hα and Hβ line profiles. After one or two iterations we found no change in the solution which gives for star A $T_{\rm eff} = 7250$ K, $\log g = 3.5$ for the $H\alpha$ line and $T_{\rm eff} = 7500$ K, $\log g = 4.0$ for Hβ. The Hα line is contaminated with several sharp telluric lines. We adopt $T_{\rm eff} = 7400 \pm 300$ K, $\log g = 4.0 \pm 0.3$ which is obtained by fitting both lines simultaneously. Lowering the adopted effective temperatures of the B and C components to $T_{\rm eff} = 5000$ K has the effect of slightly increasing $T_{\rm eff}$ of A to about 7500 K while decreasing the surface gravity to $\log g \approx 3.0$.

Using the adopted values for star A and still fixing $T_{\rm eff} = 6000$ K, $\log g = 4.5$ for components B and C, we proceeded to fine tune the relative brightnesses. The relative peak heights in the cross-correlation function are sensitive to the values chosen for the relative brightnesses, so these important quantities can be determined quite accurately. However, they do depend on the adopted value of $v \sin i$ for B and C. By varying all parameters, we found a best fit for the values listed in Table 2. The observed cross-correlation function is compared with the synthetic cross-correlation function in Fig. 3. The match between observed and synthetic spectra in the Hβ region for the parameters listed in Table 2 is shown in Fig. 4. In this figure we also show part of the spectrum after removing the contribution of star A.

We measured the equivalent widths of as many unblended Fe lines as possible in the wavelength region 6000–6800Å. A total of 22 lines were identified and measured for both stars. A microturbulence of 1 km s^{-1} was assumed. The effective temperature for each star was adjusted until there was no abundance trend with excitation potential. This yielded $T_{\rm eff} = 6000 \pm 300$ K for star B, $T_{\rm eff} = 5900 \pm 300$ K for star C. The surface gravity was then adjusted to bring the ionization balance between Fe I and Fe II into agreement. This indicated $\log g = 4.5 \pm 0.3$ dex for both stars. The iron abundances for the two stars were found to be [Fe/H] $= -0.07 \pm 0.30$ and -0.10 ± 0.26, respectively. The projected rotational velocities for B and C are close to zero; the fit to the cross-correlation function suggests $v \sin i \approx 5$ km s^{-1}. A macroturbulence of $\xi = 3$ km s^{-1} was adopted based on the Bruntt et al. (2010) calibration. An upper limit of $\xi \lesssim 5$ km s^{-1} appears to be reasonable.

We have not been able to find any sign of Ap or Am characteristics in the bright A-type star, but this would in any case be very difficult to detect in such a broad-lined star. Abt & Morrell (1995) find that all rapid rotators have normal spectra and nearly all slow rotators have abnormal spectra (Ap or Am). There does not seem to be any spectral peculiarities in the B and C companions. The lines due to

Table 2. Parameters for the three components in the spectrum. For each star, the effective temperature $T_{\rm eff}$ (K), gravity $\log g$, projected rotational velocity $v \sin i$ (km s^{-1}), metal abundance [Fe/H], radial velocity V_r (km s^{-1}) and relative brightnesses, $l/l_{\rm tot}$, are listed. Estimates of mass, radius and luminosity for the A component are from the calibration of Torres et al. (2010). Stars B and C are assumed to have approximately solar values.

	A	B	C
$T_{\rm eff}$	7400 ± 200	6000 ± 300	5900 ± 300
$\log g$	4.0 ± 0.3	4.5 ± 0.3	4.5 ± 0.3
$v \sin i$	220 ± 5	5 ± 5	5 ± 5
[Fe/H]		-0.07 ± 0.30	-0.10 ± 0.26
V_r	-10.0 ± 2	-7.0 ± 0.5	-50.9 ± 0.5
$l/l_{\rm tot}$	0.880 ± 0.01	0.066 ± 0.01	0.054 ± 0.01
$M/M_\odot$	1.7 ± 0.3	≈ 1.0	≈ 1.0
$R/R_\odot$	2.2 ± 0.9	≈ 1.0	≈ 1.0
$\log(L/L_\odot)$	1.1 ± 0.4	≈ 0.0	≈ -0.1

stars B and C appears weaker in the blue compared to the red, as would be expected from the temperature difference.

4 STELLAR PARAMETERS FROM PHOTOMETRY

We have used broad-band photometry from TYCHO-2, USNO-B1.0 R-mag., TASS-I, CMC14 r' and 2MASS to estimate the total observed bolometric flux. The Infrared Flux Method (IRFM) (Blackwell & Shallis 1977) was then used with 2MASS magnitudes to determine $T_{\rm eff}$. This gives $T_{\rm eff} = 7030 \pm 150$ K, which is somewhat smaller, but consistent with, the spectroscopic value.

The spectrum reveals strong interstellar Na D lines with $V_r = -18 \pm 1\,{\rm km\,s^{-1}}$, and an equivalent width EW = 0.15±0.02 Å. Using the Munari & Zwitter (1997) relation we estimate E(B-V) = 0.05±0.01. This raises the effective temperature determined from the IRFM to $T_{\rm eff} = 7380 \pm 160$ K, which is in good agreement with that estimated from Balmer line spectroscopic fitting.

The IRFM might be affected by the presence of cool companions (Smalley 1993). The modified IRFM would increase the effective temperature of the primary to about $T_{\rm eff} \approx 8000$ K for two main-sequence companions (both with $T_{\rm eff} \approx 6000$ K), if the primary is also main-sequence, but to no more than about 7600 K for a more evolved primary with $R \approx 3R_\odot$. This suggests that the bright A star might be somewhat evolved with $\log g \lesssim 4.0$ dex.

Fig. 5 shows the location of the three stars in the HR diagram based on our limited knowledge of their parameters. The evidence suggests that star A is slightly evolved. We have assumed that stars B and C are on the zero-age main sequence. If the three stars are gravitationally bound, as seems likely, they should also be coeval. However, the errors in the parameters are such that this cannot be tested. If we take the relative brightnesses of the three stars into account and assume that B and C are on the ZAMS, then for star A $\log L/L_\odot \approx 1.1$, which agrees with the deduced spectroscopic value.

5 FREQUENCIES

There are several hundred significant frequencies that can be extracted from the *Kepler* SC photometry. Although the inclusion of the data from Q3.3 does allow the frequencies to be refined, the large gap between this data set and the Q9 SC data leads to a complex window function. We decided to omit Q3.3 and use only the combined Q9 SC data (97.5 d) for the purpose of frequency extraction. In Table 3 we list some of the frequencies with highest amplitudes. Most of the variability is confined to the range 15–45 $\rm d^{-1}$, but there are quite a number of highly-significant low frequencies as well.

The variability is dominated by a mode at $f_1 = 22.07\ \rm d^{-1}$ with amplitude $A_1 = 1.37$ mmag. In spite of the dominance of this mode, there is no indication of harmonics. There is a peak very close to $2f_1$, but its amplitude is only about 5 micromags and its significance is doubtful. The long-cadence data (see Table 5 for a log of the observations) is useful for testing long-term amplitude variations.

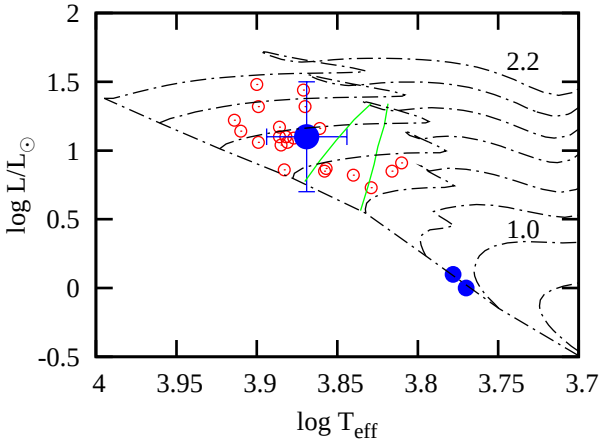

Figure 5. Possible locations of the three components in the KIC 4840675 system in the HR diagram (filled circles). The zero-age main sequence and several evolutionary sequences with solar composition (Bertelli et al. 2008) are shown. The sequences are spaced at intervals of $0.2M_\odot$ with masses of two tracks labeled. The solid lines mark the approximate location of the γ Dor variables.

Table 3. Frequencies, f_N (in $\rm d^{-1}$) and amplitudes, A_N (in millimagnitudes) of modes in KIC 4840675. The numbers in brackets are the two last digits of the standard deviations. Only frequencies with the highest amplitudes are listed.

N	f_N	A_N	N	f_N	A_N
1	22.06872(01)	1.3715(09)	21	7.94407(02)	0.0625(09)
2	33.81286(01)	0.2936(09)	22	6.96310(01)	0.0614(09)
3	23.44574(01)	0.2551(09)	23	20.07914(01)	0.0614(09)
4	24.97014(01)	0.2529(09)	24	26.63867(02)	0.0553(09)
5	16.39243(01)	0.2260(09)	25	18.10069(02)	0.0529(09)
6	27.22668(01)	0.2179(09)	26	31.56580(02)	0.0507(09)
7	30.01549(01)	0.1942(09)	27	11.23126(02)	0.0502(09)
8	19.90851(01)	0.1664(09)	28	28.71056(02)	0.0503(09)
9	21.24281(01)	0.1415(09)	29	28.19591(02)	0.0492(09)
10	31.36071(01)	0.1223(09)	30	0.11758(02)	0.0454(09)
11	30.34339(01)	0.1075(09)	31	5.29624(02)	0.0444(09)
12	18.54189(01)	0.1052(09)	32	24.32143(02)	0.0436(09)
13	21.40450(01)	0.0954(09)	33	17.10252(02)	0.0422(09)
14	27.99361(01)	0.0889(09)	34	43.26449(02)	0.0420(09)
15	21.10408(01)	0.0875(09)	35	4.50995(02)	0.0393(09)
16	22.20490(01)	0.0854(09)	36	23.99176(02)	0.0392(09)
17	42.52881(01)	0.0837(09)	37	42.75982(02)	0.0369(09)
18	20.70656(01)	0.0829(09)	38	24.15737(02)	0.0362(09)
19	2.64929(01)	0.0731(09)	39	37.61171(02)	0.0355(09)
20	21.73407(01)	0.0727(09)	40	25.99328(02)	0.0351(09)

The amplitude of this mode is clearly variable as can be seen in Fig.6 where the amplitude at each data set is shown. There appear to be smaller amplitude variations for some other modes, but these are less clear and less regular than for f_1. Nevertheless, these are probably real as they are uncorrelated with each other and therefore cannot be ascribed to instrumental effects. Amplitude variations are quite common in δ Sct stars. After prewhitening the dominant frequency, two side lobes, separated by about $0.06\ \rm d^{-1}$ from the prewhitened main peak, remain. This may be a result of the

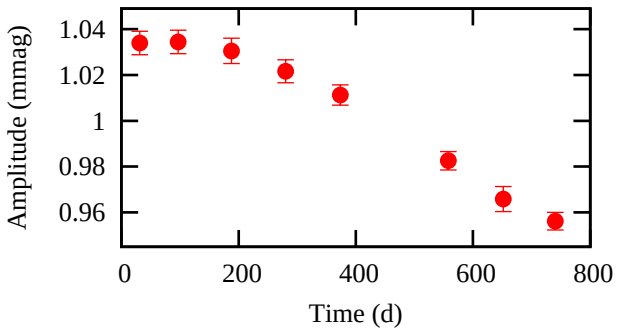

Figure 6. The amplitude of the dominant mode, f_1, as a function of time from long-cadence data.

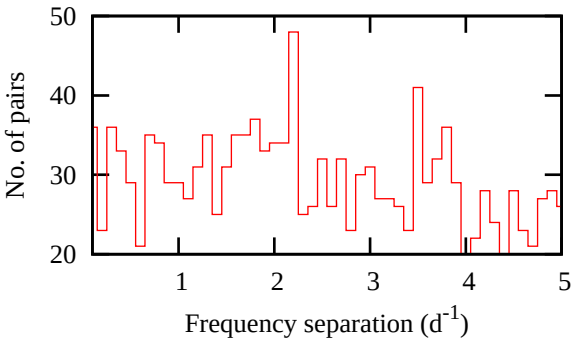

Figure 7. Histogram showing numbers of frequency pairs with the given frequency separation.

long-term amplitude variability. There are a large number of other modes with amplitudes in the range 0.05–0.20 mmag.

Without mode identification, which is not likely to be available in the foreseeable future due to the low amplitude, there is little information that can be extracted from these frequencies. However, there does seem to be a preferred separation. We have calculated all possible separations between pairs of modes in the frequency range 5–50 d^{-1} and with amplitudes greater than 0.01 mmag. The distribution of separations shows a peak at 2.2 d^{-1} and, perhaps, a lower peak at about 3.4 d^{-1} (Fig. 7). Out of 528 frequency pairs examined, 48 pairs are found with a separation of 2.20 ± 0.05 d^{-1}.

The concentration of modes having this separation may reflect rotational splitting, but without further evidence this cannot be verified. Note that even in rapidly-rotating stars, where the frequency multiplets due to rotational splitting are not equally spaced, equal frequency spacing is still preserved between modes with positive and negative values of the same azimuthal number, m, and remains $2m$ times the rotation rate (Deupree 2011). In this regard, we note that the dominant low frequency, $f_{19} = 2.649$ d^{-1}, is possibly the rotational frequency of star A (see below). Rotational splitting should be close, but not identical, to the rotational frequency. The peak frequency in the distribution of Fig 7 seems to satisfy this condition.

Balona & Dziembowski (2011) found that about 10 percent of *Kepler* δ Sct stars have one dominant mode, often with a side peak of lower amplitude. KIC 4840675 may be regarded as belonging to this group. These stars appear to obey a period - luminosity and period - temperature relationship, suggesting that the high-amplitude mode has the same spherical harmonic degree, l, in all stars. This is likely to be $l = 0$ not only because of the high amplitude, but also because rotational effects would tend to destroy any correlation between frequency and luminosity or temperature. It is therefore interesting to consider the implications if we assume that f_1 is the fundamental radial mode in KIC 4840675.

Models of δ Scuti stars with masses in the range $1.3 < M/M_\odot < 2.5$ were constructed using the Warsaw - New Jersey code. These non-rotating models use OPAL opacities, no core overshoot and a mixing length, $\alpha = 1.0$. Pulsation frequencies for each model were obtained using the `nadrot` code (Dziemblowski 1977). The average large separation, $\Delta\nu$, for unstable modes was calculated from frequencies of sequential $\ell = 0$ and $\ell = 1$ modes for all models on the zero-age main sequence until the end of core hydrogen burning. A reasonably tight correlation between $\Delta\nu$ and $\log g$ is found. A least squares fit, which includes both $\ell = 0$ and $\ell = 1$, is given by

$$\log \Delta\nu = -2.4948 + 0.7656 \log g$$

where $\Delta\nu$ is in d^{-1}. The frequency of the fundamental radial mode, f_{01}, as a function of surface gravity is well represented by

$$\log f_{01} = -2.0637 + 0.7865 \log g,$$

where f_{01} is in d^{-1}. If we assume that f_1 is the fundamental radial mode, we obtain $\log g \approx 4.3$ and $\Delta\nu \approx 6.6$ d^{-1}. The surface gravity is certainly consistent with the spectroscopic value. Thus our assumption that f_1 is the fundamental radial mode appears to be at least consistent with what we know of the star.

6 HIGH FREQUENCIES

Of particular interest is the presence of three high-frequency peaks at around 120 d^{-1}, as shown in the top panel of Fig. 2 and listed in Table 4. To prevent confusion with the δ Scuti frequencies, which we label by f_N, we label these high frequencies as ν_N. The three frequencies form a triplet with nearly equal spacing: $\nu_1 - \nu_2 = 5.371$, $\nu_3 - \nu_2 = 5.230$ d^{-1}. Notice that the separation is about $2f_{19}$, though the significance of this observation (if any) is unknown. According to the the Lomb-Scargle false alarm probability (Scargle 1982), the peaks are highly significant. In any case, there is little doubt of their reality because all three frequencies are clearly seen in periodograms of independent subsets of the data (Fig. 8). None of these frequencies can be attributed to an harmonic of f_1 or a combination frequency.

The individual peaks are shown in more detail in Fig. 9. The window function has the same shape as the peaks, which means that the high frequency peaks disappear completely when prewhitened. This indicates that they are stable frequencies with long lifetimes. Significant frequency or amplitude variations, as might occur for stochastically-excited modes would leave a residual signal after prewhitening. However, such a residual signal might still be present at the level of the background noise.

Although frequencies larger than 100 d^{-1} are seen in a

Table 4. Frequencies, ν_N, and amplitudes, A_N (in millimagnitudes) of the three high-frequency peaks.

N	$\nu_N(\mathrm{d}^{-1})$	ν_N (μHz)	A_N
1	129.031(4)	1493.41(04)	0.0058(06)
2	123.801(4)	1432.88(05)	0.0054(06)
3	118.430(5)	1370.72(06)	0.0044(05)

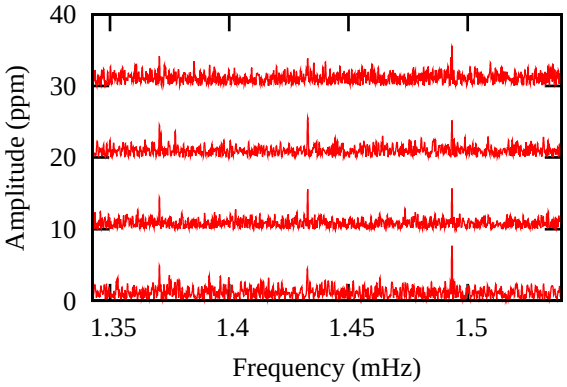

Figure 8. Periodograms in the high-frequency region for different independent data subsets. All three peaks appear in each subset.

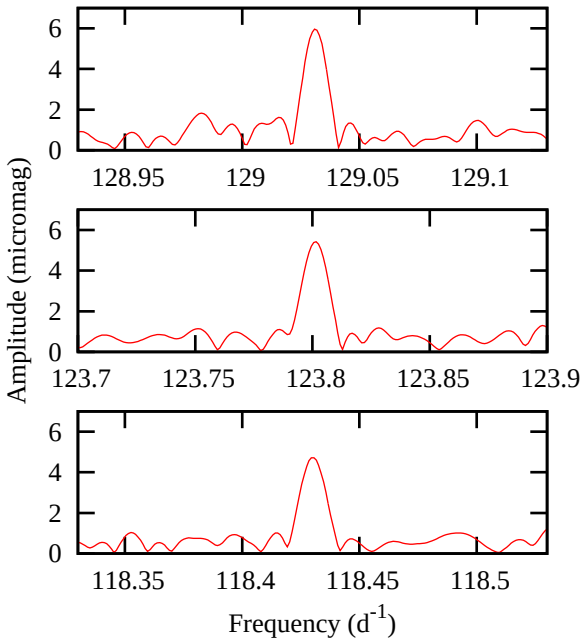

Figure 9. Detail of the periodogram in the region of the three high frequencies.

few *Kepler* δ Sct stars, they can invariably be attributed to harmonics of a dominant frequency. In KIC 4840675 this is clearly not the case, nor can they be explained as a combination of lower-frequency modes. Therefore we need to consider the excitation mechanism which can lead to such a high frequency. Since the normal κ mechanism acting in the He II ionization zone is not capable of destabilizing such high frequencies (Balona & Dziembowski 2011), we can only suppose that they must be a result of another mechanism. We know of only two mechanisms which could give rise to these frequencies: stochastic excitation of solar-like oscillations or oscillations of the roAp type. If we admit the presence of an unseen white dwarf in the system, it is also possible that the high frequencies may be a result of pulsations in a ZZ Cet, V777 Her or sdB star.

Solar-like oscillations have been suggested to explain some modes in the Am star HD 187547 (Antoci et al. 2011). The problem is that there is no simple method of discriminating between different driving mechanisms. In the case of HD 187547, the modes attributed to driving by solar-like oscillations are only of moderately high frequency (around 65 d^{-1}). Although independent modes in this frequency range are not common, they certainly exist in many *Kepler* δ Sct stars (Balona 2011). Therefore, driving by the standard κ mechanism cannot be ruled out. One of the problems in attributing the oscillations in HD 187547 to stochastically-excited modes is that the star has a relatively high effective temperature ($T_{\rm eff}$ = 7500 K), which is too hot for the star to have a significant convective zone. It is also strange that this is the only δ Sct star with solar-like oscillations, whereas there are a large number of cooler δ Sct stars in which there is no evidence for such oscillations (Balona & Dziembowski 2011).

A test for solar-like oscillations is that they have quite short lifetimes, but the high frequencies are stable to within the noise limits, so their lifetimes must about as long as the duration of the time series (90 d). Furthermore, in all other stars where solar-like oscillations are present, there is a fairly dense comb-like spectrum of modes within a symmetric amplitude envelope centered at a frequency $\nu_{\rm max}$. On the contrary, in KIC 4840675 we see only three isolated modes. If these are the highest-amplitude peaks then it is reasonable to assume that the frequency separation of about 61 μHz is the large separation.

These arguments are not sufficient to rule out solar oscillations in star A, though this seems very unlikely. The star has a mass of about 1.7$\mathrm{M}_\odot$ and a radius of about 2.2$\mathrm{R}_\odot$. From a comparison with a grid of models with various chemical compositions and core overshooting using ASTEC (Christensen-Dalsgaard 2008b) and ADIPLS (Christensen-Dalsgaard 2008a), we find a large separation $\Delta\nu \approx 54\,\mu$Hz. This, in turn results in maximum power at $\nu_{\rm max} \approx 990\,\mu$Hz from the scaling relationship of Stello et al. (2009), which is significantly lower than observed. On the other hand, if we look for models with $\Delta\nu \approx 60\mu$Hz, similar to the separation between peaks, and $T_{\rm eff}$ = 7400 K, we find a slightly lower luminosity, $\log L/L_\odot \approx 1.03$. From the same scaling relationship we obtain $\nu_{\rm max} \approx 1130\mu$Hz, which is still significantly lower than observed. We conclude that it would be difficult to understand both the location of the high frequencies and their separation if they are due to solar-like pulsations in star A.

If the high frequencies are a result of solar-like oscillations in either star B or C, their real amplitudes must be about ten times larger or about 50 ppm. There is a strong correlation between amplitude and $\nu_{\rm max}$ in *Kepler* stars with

solar-like oscillations (Huber et al. 2011). The expected amplitude for $\nu_{\rm max} \approx 1450\mu$Hz is only 2 ppm, which is far larger than the expected value of 50 ppm. On this basis alone, it is clear that the high-frequency modes are most unlikely to be solar-like oscillations in one of the two faint companion stars.

The stellar parameters for B and C are even more uncertain than for A, but they do seem to be quite similar to the Sun. However, $\nu_{\rm max} = 3300\mu$Hz in the Sun is much larger than observed in KIC4840675. If we use the parameters in Table 2 for components B and C, the tight scaling relationship between $\Delta\nu$ and $\nu_{\rm max}$ (Stello et al. 2009) results in values for $\nu_{\rm max}$ that are even larger than that of the Sun. For the Sun, $\Delta\nu = 135\mu$Hz, which is also much larger than the separation between the frequency triplets. We conclude that although spectroscopy indicates that the two faint companions are similar to the Sun, the expected frequency and large separation are very different from the observed values. This, together with the fact that the observed amplitude of solar-like oscillations is at least an order of magnitude larger than expected, rules out solar-like oscillations in B and C as an explanation for the high frequencies.

Let us now turn to the possibility that the high frequencies are caused by roAp-like pulsations. Star A is not an Ap star, so they cannot be described as roAp pulsations, but any mechanism which suppresses convection could, in principle, lead to the excitation of high-frequency oscillations through the opacity mechanism working on the H ionization region. In the presence of a strong magnetic field, convection is expected to be suppressed in the magnetic polar regions, rendering high frequency modes overstable in the region of the HR diagram where roAp stars are observed (Cunha 2002).

To test this possibility, we used non-adiabatic models with and without suppression of envelope convection. A non-local, time-dependent mixing-length formalism was used (Gough 1977). In the models with envelope convection, no high radial order high-frequency modes are excited. When convection is suppressed, both low radial order and high radial order modes are excited. In fact, the region of frequencies in which modes are found to be excited is similar to the region of the high frequencies in KIC 4840675. In addition, this model has a large separation similar to the observed separation between the high-frequency triplets. Despite this, the large rotational velocity derived for the A component makes this star very different from all other roAp stars known (and a faster rotator than any Ap stars known to date), making this scenario rather unlikely.

Finally, we always need to bear in mind that there might be a faint star in the system which may be responsible for the high-frequency oscillations. Pulsating white dwarfs, such as ZZ Cet or V777 Her stars, have frequencies in the observed range as do subdwarf B stars (sdB stars). Observations in the far UV may be able to detect the presence of a white dwarf in the system, but unfortunately the star was not observed in the *GALEX* survey (`http://galex.stsci.edu/GR6/`). The luminosity of a white dwarf is about $10^{-2} - 10^{-3} L_\odot$ while the total luminosity of the three components in the KIC 4840675 system is about $12L_\odot$. Therefore the amplitude of the white dwarf pulsations would be about $10^3 - 10^4$ larger in the absence of the three components, or about 0.5–5.0 mmag, which is well within the observed range of ZZ Cet or V777 Her stars.

Table 5. Log of *Kepler* long-cadence observations for KIC 4840675. The *Kepler* quarter name, the start and ending truncated Julian day, the duration and the number of data points, N, are shown.

Quarter	Julian day	Days	N
Q0	54953.5 - 54963.2	9.7	476
Q1	54964.5 - 54998.0	33.5	1639
Q2	55002.5 - 55091.5	88.9	4194
Q3	55093.2 - 55182.5	89.2	4228
Q4	55185.4 - 55275.2	89.8	4159
Q5	55276.5 - 55371.2	94.7	4538
Q7	55463.2 - 55552.5	89.4	4295
Q8	55568.4 - 55635.3	66.9	3143
Q9	55641.5 - 55738.9	97.4	4703

In conclusion, none of the three stars in the system is an obvious candidate for the origin of the high frequency oscillations. While it is possible that the high frequencies could arise in an unobserved white dwarf companion, this remains a pure conjecture until the putative white dwarf is observed. Until then, the nature of the high frequencies must remain unresolved.

7 LOW FREQUENCIES

Since the advent of *Kepler* we know that δ Scuti stars nearly always have low frequencies. This is a general feature in all A–F stars and not only in δ Sct variables. It seems that the dominant low frequency is very often the rotational frequency (Balona 2011). Because low frequencies occur in the hottest A-type stars, they cannot be attributed to γ Dor pulsations. The convective blocking instability which is thought to drive γ Dor pulsations cannot act in these hot stars because they lack a substantial superficial convective zone.

We have already mentioned that KIC 4840675 has a prominent peak at $f_{19} = 2.649$ d^{-1} which may be the rotational frequency of star A. There are a number of significant peaks at harmonics of f_{19}, indicating that this low frequency variation is non-sinusoidal. For low frequencies, the LC data are very useful because they cover a much longer period, as shown by the observational log in Table 5. Again we use the uncalibrated LC data and have adjusted trends and jumps between data sets by visual inspection. The periodograms of individual LC data sets show that f_{19} and its harmonics undergo large amplitude variations.

We can extract the shape of the light curve for each quarter by removing all significant frequencies except those relating to f_{19} and its harmonics. Fig. 10 shows the resulting phase curves. It is clear from Fig. 10 that the amplitude variation in the periodogram is actually a variation in the light curve shape with time. Note that for Q7–Q9 there is an additional bump at phase $\phi = 0.6$ which is not present at earlier times. On the other hand for Q3 and Q4 the bump is at $\phi = 0.3$. One might even interpret the sequence of light curves as a stationary curve with a traveling bump. Balona (2011) finds that about 8 percent of *Kepler* A-type stars manifest clear traveling bumps in the low frequency

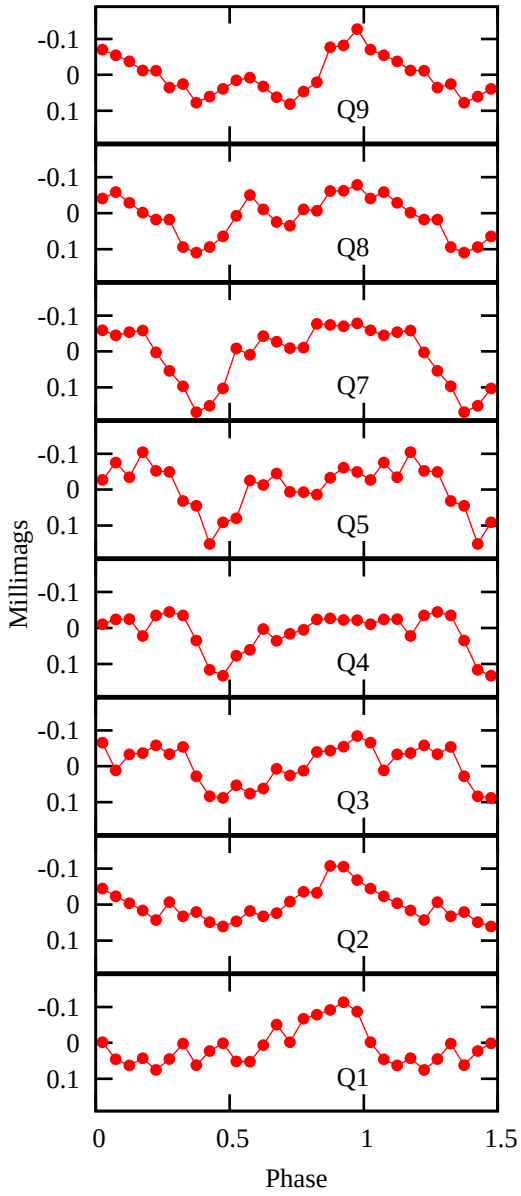

Figure 10. The light curve of long-cadence data phased with frequency $f_{19} = 2.649\ \mathrm{d}^{-1}$. All frequencies except for f_{19} and its harmonics have been removed. The epoch of phase zero is BJD 54950.00.

variation similar to those found in migrating star spots in cool stars.

We know from statistical studies of large numbers of *Kepler* A–F stars that the dominant low frequency is a measure of the rotational velocity of the star (Balona 2011). Therefore it is reasonable to assume that f_{19} represents a rotational frequency, presumably of the bright A component. The projected rotational velocity of star A implies that the equatorial velocity $v_e > 220\,\mathrm{km\,s^{-1}}$. If we assume f_{19} to be the rotational frequency, we can derive a lower bound for the stellar radius $R > 1.63 R_\odot$. From its effective temperature of 7400 K, we obtain a lower bound for the luminosity $\log L_A/L_\odot > 0.86$, which is in agreement from the estimate based on the spectroscopic parameters (Table 2).

The above arguments show that it is reasonable to suppose that f_{19} is the rotational frequency. In that case, the light curve of Fig. 10 strongly indicates that the photosphere of star A has a non-uniform brightness distribution, possibly as a result of star spots or co-rotating obscurations. It would seem that the spots or obscurations migrate or change intensity on a time scale of months. There are other indications for surface patches in A stars (Balona 2011) which might suggest a partial explanation for low frequencies in A stars.

8 FREQUENCY MODULATION IN A BINARY

If one of the components of a binary system is a pulsating star, the pulsation frequency is Doppler shifted due to the orbital motion. As a result, the periodogram shows additional frequency components. Shibahashi & Kurtz (2012) have derived general expressions for these components which enable the orbital parameters to be extracted in the same way as traditional methods using the radial velocities. In the case of a relatively rapidly rotating δ Sct star such as KIC 4840675, the photometric derivation of the mass function is more precise than is possible with spectroscopic radial velocities.

For two stars with masses m_1 and m_2 in a circular orbit with inclination i, Shibahashi & Kurtz (2012) show that the frequency modulation results in the appearance of two sidelobes spaced by the orbital frequency. They show that the mass function,

$$f(m_1, m_2, \sin i) = \frac{m_2^3 \sin^3 i}{(m_1 + m_2)^2},$$

can be expressed as

$$f(m_1, m_2, \sin i) = \left(\frac{A_{+1} + A_{-1}}{A_0}\right)^3 \frac{P_{\rm pul}^3}{P_{\rm orb}^2} \frac{c^3}{2\pi G}, \qquad (1)$$

where A_{+1}, A_{-1} and A_0 refer to the amplitudes of the components of the frequency triplet, A_0 being the amplitude of the central component. $P_{\rm pul}$ and $P_{\rm orb}$ are the pulsation and orbital periods respectively, G is the gravitational constant and c the speed of light.

For the highest amplitude mode in KIC 4840675, f_1, we have $A_0 = 1.37$ mmag (see Table 3). We do not detect any equally spaced sidelobes with amplitudes greater than 10 μmag, which is a conservative upper estimate of the detection limit. Therefore we can place firm upper limits on $A_{-1}, A_{+1} \leqslant 0.01$ mmag. We thus have

$$\frac{A_{+1} + A_{-1}}{A_0} = (\frac{2\pi G}{c^3})^{1/3} \frac{m_2 \sin i}{(m_1 + m_2)^{2/3}} \frac{P_{\rm orb}^{2/3}}{P_{\rm pul}} < 0.01$$

Assuming that $m_1 = 1.7\,\mathrm{M}_\odot$ for the A star and $m_2 = 2\,\mathrm{M}_\odot$ for the sum of the masses of the two other components, we find for $P_{\rm orb} = 10$ d and $i = 90^\circ$ that $A_{+1} + A_{-1}/A_0 = 0.06 \sin i$. From the lack of any frequency triplets about f_1 we can thus rule out all but the smallest of inclinations ($i < 14^\circ$). For longer orbital periods, up to the length of the data set of nearly 800 d, the constraint is much more stringent. For an orbital period of 500 d, for example, $A_{+1} + A_{-1}/A_0 = 0.78 \sin i$. In this case it is possible to detect the sidelobes in the mode of highest amplitude for $i > 1^\circ$.

In general, A stars with orbital periods less than 10 d, have synchronous orbits and $v \sin i < 100\,\mathrm{km\,s^{-1}}$. The lack

of sidelobes to the main frequency in KIC 4840675 thus precludes a short orbital period. As long as the orbit of star A about the other two stars is not nearly face-on, the orbital period must be longer than the length of the data set (785 d). Given the same constraints on orbital period and inclination, one can rule out a roAp star in the system in addition to the three known components. In any case, such a star would be relatively luminous and easily detected in the spectrum.

9 CONCLUSIONS

We show that KIC 4840675 is at least a triple system. The brightest component is a rapidly-rotating main sequence A star which is also a δ Sct variable. The other two stars are similar to the Sun. The most unusual feature of this stellar system is the presence of three independent pulsation modes with frequencies of 118, 124 and 129 d^{-1}. These frequencies are much higher than observed in any other δ Sct star and cannot be explained by the same mechanism which drives the δ Sct pulsations.

We considered two possible mechanisms: solar-like modes excited by convection or self-excited modes of the roAp type. The frequency pattern does not resemble the comb-like structure seen in other stars with solar-like oscillations. Moreover, the mode lifetime appears to be longer than expected for solar-like modes. We find that the observed high frequencies and implied large separation cannot be matched for solar-like modes in star A. The amplitude of the high-frequency oscillations is far too large to be attributed to stars B and C. Furthermore, the same problems of matching the frequencies and large separation exists as for star A. We thus concluded that the high frequencies cannot be due to solar-like oscillations in any of the three stars.

In spite of the fact that star A cannot be an Ap star, we found that models of roAp pulsation do agree quite well with the observed frequencies and frequency spacing. Unless a strong magnetic field is detected in this star, the possibility that this is a new type of roAp-like variable is difficult to accept at this stage. Since none of the three stars seem obvious candidates for the high frequencies, the only alternative is to attribute the origin of these frequencies to an unseen compact companion. However, until such time that the compact companion is detected, this must remain a conjecture.

We find several low frequencies in the light curve which is typical of all A–F stars when observed with high photometric precision. It has been shown that the dominant low frequency in A–F stars is probably the rotational frequency (Balona 2011). Indeed, the dominant low frequency in KIC 4840675 has several harmonics which supports rotational modulation rather than a pulsation. Furthermore, the frequency is consistent with the expected rotational frequency of the star. The light curve changes from season to season, suggesting migrating star spots or spots which change intensity with time.

Further progress in locating the origin of the high frequencies could be made if photometry in the far UV were available. This might reveal the presence of a compact companion. Until then, KIC 4840675 remains a puzzle and a challenge to our understanding of stellar pulsations.

ACKNOWLEDGMENTS

The authors wish to thank the *Kepler* team for their generosity in allowing the data to be released to the Kepler Asteroseismic Science Consortium (KASC) ahead of public release and for their outstanding efforts which have made these results possible. Funding for the *Kepler* mission is provided by NASA's Science Mission Directorate.

LAB wishes to express his sincere thanks to the South African Astronomical Observatory and the National Research Foundation for financial support. R. Sz. has been supported by the Hungarian OTKA grants K83790 and MB08C 81013, the 'Lendület' program and the János Bolyai Research Scholarship of the Hungarian Academy of Sciences. This investigation has been supported by the Austrian Fonds zur Förderung der wissenschaftlichen Forschung through project P 21830-N16 (MB). MSC is supported by a Ciência 2007 contract and the project PTDC/CTEAST/098754/2008, funded by FCT (Portugal) and POPH/FSE (EC).

REFERENCES

Abt H. A., Morrell N. I., 1995, ApJS, 99, 135
Antoci V., Handler G., Campante T. L., Thygesen A. O., Moya A., Kallinger T., Stello D., Grigahcène A., Kjeldsen H., Bedding T. R., Lüftinger T., Christensen-Dalsgaard J., Catanzaro G., Frasca A., De Cat P., Uytterhoeven K., Bruntt H., Houdek G., Kurtz D. W., Lenz P., Kaiser A., van Cleve J., Allen C., Clarke B. D., 2011, Nature, 477, 570
Balmforth N. J., Cunha M. S., Dolez N., Gough D. O., Vauclair S., 2001, MNRAS, 323, 362
Balona L. A., 2011, MNRAS, 415, 1691
Balona L. A., Dziembowski W. A., 2011, MNRAS, 417, 591
Baran A., 2012, Spurious Frequencies in SC Data. Kepler Data Release 12 Notes
Benkő J. M., Szabó R., Paparó M., 2011, MNRAS, 417, 974
Bertelli G., Girardi L., Marigo P., Nasi E., 2008, A&A, 484, 815
Blackwell D. E., Shallis M. J., 1977, MNRAS, 180, 177
Brown T. M., Latham D. W., Everett M. E., Esquerdo G. A., 2011, AJ, 142, 112
Bruntt H., Bedding T. R., Quirion P.-O., Lo Curto G., Carrier F., Smalley B., Dall T. H., Arentoft T., Bazot M., Butler R. P., 2010, MNRAS, 405, 1907
Castelli F., Gratton R. G., Kurucz R. L., 1997, A&A, 318, 841
Christensen-Dalsgaard J., 2008a, Ap&SS, 316, 113
—, 2008b, Ap&SS, 316, 13
Cunha M. S., 2002, MNRAS, 333, 47
Deupree R. G., 2011, ApJ, 742, 9
Draper P. W., Allan A., Berry D. S., Currie M. J., Giaretta D., Rankin S., Gray N., Taylor M. B., 2005, in Astronomical Society of the Pacific Conference Series, Vol. 347, Astronomical Data Analysis Software and Systems XIV, P. Shopbell, M. Britton, & R. Ebert, ed., p. 22
Dziemblowski W., 1977, Acta Astronomica, 27, 95
Gilliland R. L., Jenkins J. M., Borucki W. J., Bryson S. T., Caldwell D. A., Clarke B. D., Dotson J. L., Haas M. R.,

Hall J., Klaus T., Koch D., McCauliff S., Quintana E. V., Twicken J. D., van Cleve J. E., 2010, ApJ, 713, L160
Gough D. O., 1977, ApJ, 214, 196
Gray R. O., 2010, A stellar spectral synthesis program. www1.appstate.edu/dept/physics/spectrum/spectrum.html
Guzik J. A., Kaye A. B., Bradley P. A., Cox A. N., Neuforge C., 2000, ApJ, 542, L57
Huber D., Bedding T. R., Stello D., Hekker S., Mathur S., Mosser B., Verner G. A., Bonanno A., Buzasi D. L., Campante T. L., Elsworth Y. P., Hale S. J., Kallinger T., Silva Aguirre V., Chaplin W. J., De Ridder J., García R. A., Appourchaux T., Frandsen S., Houdek G., Molenda-Żakowicz J., Monteiro M. J. P. F. G., Christensen-Dalsgaard J., Gilliland R. L., Kawaler S. D., Kjeldsen H., Broomhall A. M., Corsaro E., Salabert D., Sanderfer D. T., Seader S. E., Smith J. C., 2011, ApJ, 743, 143
Jenkins J. M., Caldwell D. A., Chandrasekaran H., Twicken J. D., Bryson S. T., Quintana E. V., Clarke B. D., Li J., Allen C., Tenenbaum P., Wu H., Klaus T. C., Van Cleve J., Dotson J. A., Haas M. R., Gilliland R. L., Koch D. G., Borucki W. J., 2010, ApJ, 713, L120
Koen C., Kurtz D. W., Gray R. O., Kilkenny D., Handler G., Van Wyk F., Marang F., Winkler H., 2001, MNRAS, 326, 387
Kurtz D. W., 1982, MNRAS, 200, 807
Michaud G., 1970, ApJ, 160, 641
Munari U., Zwitter T., 1997, A&A, 318, 269
Pinsonneault M. H., An D., Molenda-Żakowicz J., Chaplin W. J., Metcalfe T. S., Bruntt H., 2011, ArXiv e-prints
Saio H., 2005, MNRAS, 360, 1022
Scargle J. D., 1982, ApJ, 263, 835
Shibahashi H., Kurtz D. W., 2012, ArXiv e-prints
Smalley B., 1993, MNRAS, 265, 1035
Stello D., Chaplin W. J., Basu S., Elsworth Y., Bedding T. R., 2009, MNRAS, 400, L80
Torres G., Andersen J., Giménez A., 2010, A&A Rev., 18, 67
Uytterhoeven K., Moya A., Grigahcène A., Guzik J. A., Gutiérrez-Soto J., Smalley B., Handler G., Balona L. A., Niemczura E., Fox Machado L., Benatti S., Chapellier E., Tkachenko A., Szabó R., Suárez J. C., Ripepi V., Pascual J., Mathias P., Martín-Ruíz S., Lehmann H., Jackiewicz J., Hekker S., Gruberbauer M., García R. A., Dumusque X., Díaz-Fraile D., Bradley P., Antoci V., Roth M., Leroy B., Murphy S. J., De Cat P., Cuypers J., Kjeldsen H., Christensen-Dalsgaard J., Breger M., Pigulski A., Kiss L. L., Still M., Thompson S. E., van Cleve J., 2011, A&A, 534, A125